Electrostatic Interaction of Internal Mg^{2+} with Membrane PIP_2 Seen with KCNQ K^+ Channels

Byung-Chang Suh and Bertil Hille

Department of Physiology and Biophysics, University of Washington School of Medicine, Seattle, WA 98195

Activity of KCNQ (Kv7) channels requires binding of phosphatidylinositol 4,5-bisphosphate (PIP_2) from the plasma membrane. We give evidence that Mg^{2+} and polyamines weaken the KCNQ channel–phospholipid interaction. Lowering internal Mg^{2+} augmented inward and outward KCNQ currents symmetrically, and raising Mg^{2+} reduced currents symmetrically. Polyvalent organic cations added to the pipette solution had similar effects. Their potency sequence followed the number of positive charges: putrescine (+2) < spermidine (+3) < spermine (+4) < neomycin (+6) < polylysine (>>+6). The inhibitory effects of Mg^{2+} were reversible with sequential whole-cell patching. Internal tetraethylammonium ion (TEA) gave classical voltage-dependent block of the pore with changes of the time course of K^+ currents. The effect of polyvalent cations was simpler, symmetric, and without changes of current time course. Overexpression of phosphatidylinositol 4-phosphate 5-kinase Iγ to accelerate synthesis of PIP_2 attenuated the sensitivity to polyvalent cations. We suggest that Mg^{2+} and other polycations reduce the currents by electrostatic binding to the negative charges of PIP_2, competitively reducing the amount of free PIP_2 available for interaction with channels. The dose–response curves could be modeled by a competition model that reduces the pool of free PIP_2. This mechanism is likely to modulate many other PIP_2-dependent ion channels and cellular processes.

The Journal of General Physiology

INTRODUCTION

Phosphatidylinositol 4,5-bisphosphate (PIP_2) is a minor but essential signaling lipid that is needed for many plasma membrane processes, including the function of ion channels and transporters, control of endocytosis, and the nucleation of cytoskeletal networks (Hilgemann et al., 2001; Suh and Hille, 2005). This paper describes the effect of intracellular Mg^{2+} on the availability of PIP_2 for ion channels, as revealed by using KCNQ channels as an indicator. M-type K^+ channels (KCNQ, Kv7) are low-threshold voltage-activated channels important in the physiology and pathophysiology of neurons, heart, and epithelia (Brown, 1988; Delmas and Brown, 2005; Lerche et al., 2005). They control the membrane potential and cell excitability and can be turned off by activating receptors that couple to PLC (Marrion et al., 1989; Bernheim et al., 1992; Jones et al., 1995; Delmas and Brown, 2005). The principal mechanism of this regulation is that the channels require PIP_2 to function and PLC depletes the essential PIP_2 from the plasma membrane (Suh and Hille, 2002; Zhang et al., 2003; Ford et al., 2004; Winks et al., 2005; Horowitz et al., 2005; Suh et al., 2006). Hence the magnitude of the current in KCNQ channels tracks the availability of PIP_2 in the plasma membrane.

Magnesium ion, the most abundant intracellular alkaline earth cation, interacts with polyvalent anions, notably with organic polyphosphates such as ATP and PIP_2. It is a necessary cofactor for protein and lipid kinases, phosphatases, and ATPases; magnesium ion helps stabilize the organization of negatively charged DNA, RNA, and membranes (Alvarez-Leefmans et al., 1987). Although the total cellular Mg^{2+} content is typically >10 mM, most of this is bound to nucleotides and nucleic acids. Mammalian cells are believed to have resting free Mg^{2+} concentrations of 0.5–1.0 mM (Gupta et al., 1984; White and Hartzell, 1989; London, 1991; Romani and Scarpa, 2000). Changes in intracellular Mg^{2+} observed in response to specific stimuli are typically considered small and slow, but the lack of good Mg^{2+} indicators might hide more interesting behavior. Some Mg^{2+}-permeable ion channels TRPM6 and TRPM7 contribute to homeostasis of intracellular Mg^{2+} (Schlingmann et al., 2002; Walder et al., 2002; Schmitz et al., 2003; Voets et al., 2004). There are reports that free $[Mg^{2+}]_i$ can rise several millimolar during the activation of some receptors (Brocard et al., 1993; Takaya et al., 1998) or as a consequence of intracellular Ca^{2+} concentration increases (Murphy et al., 1989a; Gotoh et al., 1999); and Mg^{2+} can be released from mitochondria when their membrane potential falls (Kubota et al., 2005). Cytoplasmic Mg^{2+} influences the activity of ion channels in several ways. Notably, intracellular Mg^{2+}

Correspondence to Bertil Hille: hille@u.washington.edu

Abbreviations used in this paper: IP_3, inositol 1,4,5-trisphosphate; PIP, phosphatidylinositol 4-phosphate; PIP_2, phosphatidylinositol 4,5-bisphosphate; Oxo-M, oxotremorine-M; TEA, tetraethylammonium ion; PIPKIγ, phosphatidylinositol 4-phosphate 5-kinase Iγ.

and organic polycations block outward current in some K^+ channels by voltage-dependent binding within the inner vestibule of the pore (Vandenberg, 1987; Lu and MacKinnon, 1994; Voets et al., 2003; Obukhov and Nowycky, 2005; Zhang et al., 2006). This mechanism underlies fast inward rectification. In addition, intracellular Mg^{2+} exerts "slow" inhibitory effects in KCNQ1/KCNE1 channels, TRPV5 and TRPM7 channels, and Kir2.3 (IRK3) channels (Chuang et al., 1997; Shen and Marcus, 1998; Nadler et al., 2001; Loussouarn et al., 2003; Du et al., 2004; Lee et al., 2005). Each of these is a PIP_2-requiring ion channel. Thus physiological effects of Mg^{2+} on membrane excitability merit deeper study.

Intracellular Mg^{2+} has several known roles in the receptor-mediated modulation of KCNQ channels. First, submillimolar Mg^{2+} is needed for onset and termination of G-protein signaling, where it is involved in the conformational changes leading to G-protein subunit dissociation and in the GTPase step leading to deactivation of Gα subunits (Gilman, 1987; Suh et al., 2004). Millimolar Mg^{2+} is required for the phosphoinositide kinases that restore PIP_2 pools and hence mediate M-current recovery (Yamakawa and Takenawa, 1988; Suzuki et al., 1991; Downing et al., 1996). Therefore cytoplasmic Mg^{2+} can be a limiting factor for both inhibition and recovery of KCNQ channels when the receptor is stimulated (Suh et al., 2004). In addition, one must consider the possibility of the fast block and the slow inhibition already mentioned for other channels. Here we show that internal Mg^{2+} depresses KCNQ currents. We argue that internal Mg^{2+} and other polyvalent cations regulate KCNQ channel activity by reducing the availability of PIP_2 for binding to the channel. This may correspond to the slow inhibitory mechanism reported in other channels.

MATERIALS AND METHODS

Cell Culture and Transfection

Transformed human embryonic kidney tsA-201 (tsA) cells were cultured and transiently transfected using Lipofectamine 2000 (Invitrogen) with various cDNAs (Suh et al., 2004) including mouse M_1-muscarinic receptor (1 μg, from N. Nathanson, University of Washington, Seattle, WA), the channel subunits human KCNQ2 and rat KCNQ3 (Kv7.2 and Kv7.3; 1 μg, from D. McKinnon, State University of New York, Stony Brook, NY), and when necessary, GFP (0.1 μg) as a marker for transfection. In some experiments with confocal microscopy, we monitored PIP_2 and its cleavage products by transfecting with fluorescent translocation probes, either PH-PLCδ1-EGFP (EGFP-PH_{PLC}, 0.25 μg, from P. De Camilli, HHMI, Yale University, New Haven, CT), which binds to PIP_2 and IP_3, or PKC-C1a-EGFP (GFP-$C1_{PKC}$, 0.25 μg, from T. Meyer, Stanford University, Stanford, CA), which binds to diacylglycerol. tsA cells were maintained in DMEM (Invitrogen) supplemented with 10% FCS and 0.2% penicillin/streptomycin.

Reagents and Bathing Solutions

The muscarinic receptor agonist oxotremorine-M was applied at 10 μM. Chemicals were purchased from Sigma-Aldrich. We used 30,000–70,000 MW poly-L-lysine (Sigma-Aldrich). The external Ringer's solution used for confocal microscopy and for current recording contained (in mM) 160 NaCl, 2.5 KCl, 2 $CaCl_2$, 1 $MgCl_2$, 10 HEPES, and 8 glucose, adjusted to pH 7.4 with NaOH. The high K^+ Ringer's solution contained (in mM) 132.5 NaCl, 30 KCl, 2 $CaCl_2$, 1 $MgCl_2$, 10 HEPES, and 8 glucose, adjusted to pH 7.4 with NaOH.

Confocal Imaging and Analysis

tsA cells were imaged 24–36 h after transfection on polylysine-coated coverslips (Suh et al., 2004). Images were taken every 5 s on a Leica TCS/MP confocal microscope at room temperature and processed with Metamorph (UIC) and Igor Pro 4.0 (Wavemetrics, Inc.). To obtain averaged time courses, the fluorescence intensity F over a given region of the cytoplasm or nucleus was usually normalized to the average baseline intensity for the 30 s before agonist application F_0 (F/F_0). Images are shown here in negative contrast so that the brightest fluorescence appears black.

Electrophysiology

tsA cells were whole-cell clamped at room temperature 24–48 h after transfection (Suh et al., 2004). The bath solutions exchanged in ~6 s. The standard pipette solution contained (in mM) 175 KCl, 5 $MgCl_2$, 5 HEPES, 0.1 BAPTA, 3 Na_2ATP, 0.1 Na_3GTP, pH 7.4, adjusted with KOH. This solution had a free Mg^{2+} concentration of 2.08 mM (estimated with the WinMaxC program). To vary the free Mg^{2+}, other pipette solutions contained 1, 3, and 10 mM added $MgCl_2$ or 1 mM EDTA and no added $MgCl_2$ but 0.65 mM $CaCl_2$. Pipettes were pulled to a resistance of 1.8–2.3 MΩ, and experiments were not continued if the series resistance was >3 MΩ. Series resistance was 60% compensated. Recordings were performed using a HEKA EPC-9 amplifier with Pulse software (HEKA Elektronik). Data analysis was done using Igor Pro 4.0. Cells were held at a holding potential of −20 mV, and 500-ms test pulses to −60 mV were given every 4 s. Reported values ($I_{-20\ mV}$) are mean outward current taken at −20 mV just before each step to −60 mV. Recordings started 3–5 min after breakthrough.

Student's unpaired t test (two tailed), or, when indicated, a one-way ANOVA was used to test for significance. Where error bars are shown, they represent SEM.

RESULTS

KCNQ Current Is Sensitive to Intracellular Mg^{2+} and Polyamines

We studied KCNQ K^+ currents using whole-cell recording from tsA cells transfected with KCNQ2/KCNQ3 channel subunits. Fig. 1 A shows families of outward currents obtained with depolarizing voltage steps from −70 mV at 10-mV intervals in a standard Ringer's bathing solution containing 2.6 mM K^+. The insets show currents elicited by the classic M-current deactivation voltage protocol with the membrane held at −20 mV, where KCNQ channels are open and pass a steady noninactivating current, and then stepped to −60 mV where channels deactivate, and back to −20 mV. The phenomenon we wanted to study is apparent when comparing experiments where the pipette solution contained the 5 mM control value of total Mg^{2+} (left) with those where the pipette contained EDTA and no added Mg^{2+} (right). Initially the KCNQ currents are the same in these exemplar cells, but 3 min after breakthrough, the currents have decreased with the 5 mM Mg^{2+} pipette solution, whereas they increased with the Mg^{2+}-free (EDTA) pipette so-

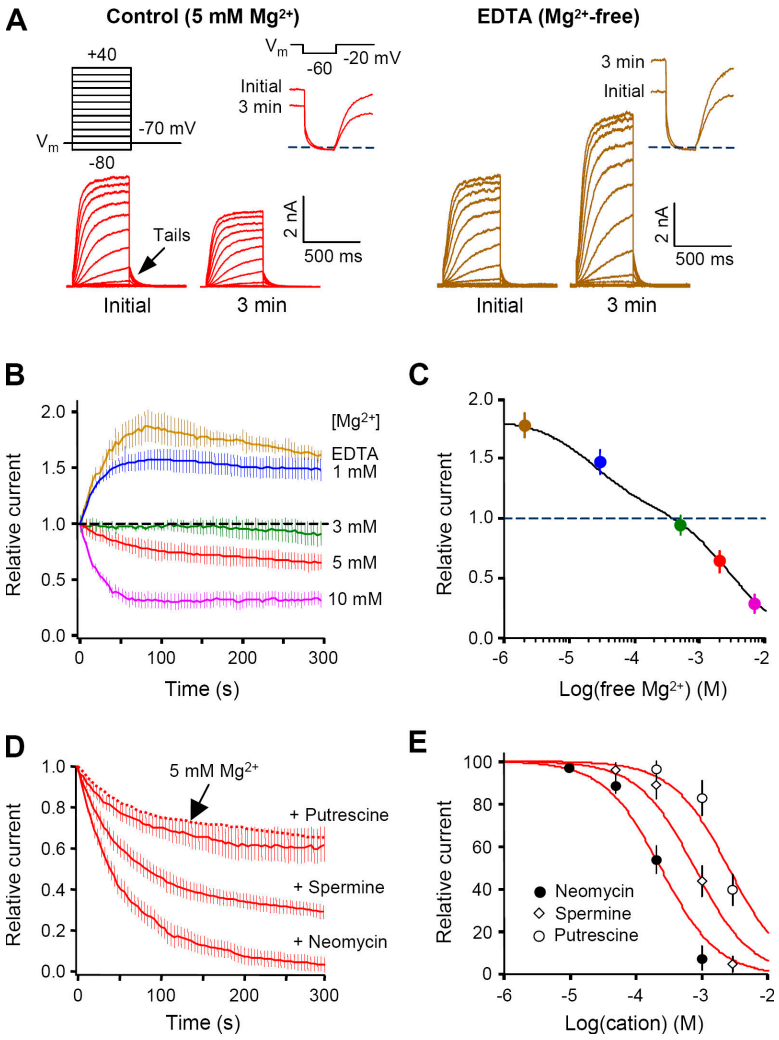

Figure 1. Modulation of KCNQ current by intracellular Mg^{2+} and polyvalent cations in tsA cells. (A) Bidirectional regulation of KCNQ current by changes of intracellular Mg^{2+} concentration. Families of current elicited by voltage steps from −80 to +40 mV, in 10-mV intervals (holding potential, −70 mV, see the pulse protocol), at the start (initial) of intracellular dialysis with 5 mM Mg^{2+} (control) or with EDTA (Mg^{2+}-free) solution, and 3 min later. Inset shows the initial current waveforms and 3 min after intracellular dialysis using the deactivation protocol (holding potential, −20 mV, see the pulse protocol). Dashed line in the current traces is the zero-current level. (B) Time course of KCNQ current changes during dialysis with various concentrations of Mg^{2+}. Data are shown as holding current at −20 mV relative to the initial level. Mean ± SEM. n = 5–12. (C) Relative current at −20 mV, 3 min after the start of dialysis vs. intracellular free Mg^{2+}. The line is calculated from equilibrium binding according to a model described in the Discussion and the Appendix. (D) Inhibition of KCNQ current by the polyvalent cations neomycin, spermine, or putrescine (all 1 mM) added to the 5 mM Mg^{2+} control pipette solution. n = 5–7. Dotted line represents the average current in the whole-cell configuration with control pipette solution. (E) Concentration dependence of inhibition by neomycin, spermine, and putrescine (measured 5 min after breakthrough). n = 3–6. The lines are calculated from the binding model referred to above.

lution. These changes in amplitude were not accompanied by shifts in the voltage dependence of channel activation (midpoint −28.3 ± 0.7 mV with 5 mM Mg^{2+} vs. −27.6 ± 0.5 mV with EDTA, n = 5) or in the rates of channel deactivation or activation (Fig. 1 A, insets). Similar Mg^{2+} dependence was seen in cells treated with the PLC inhibitor U73122 or with the phosphoinositide (PI) 4-kinase inhibitor wortmannin (unpublished data), implying that the effect was not due to alterations of PIP_2 metabolism by PLC or lipid kinases. The effect developed within a minute or two after breakthrough (Fig. 1 B), approximately the time expected for dialysis of ions from the pipette into the cytosol.

In this paper we usually give the total Mg^{2+} in the pipette solutions. Much of that becomes bound to the 3 mM ATP present. Thus, the 5 mM Mg^{2+} pipette solution has a calculated free Mg^{2+} concentration of only 2.08 mM. Plotting the relative change of current amplitude against the calculated free Mg^{2+} concentration (Fig. 1 C) reveals a graded dependence on free Mg^{2+} that crosses the null point at 0.47 mM free Mg^{2+}. This is near the range of internal free Mg^{2+} estimated for resting cells (Gupta et al., 1984; White and Hartzell, 1989; London, 1991; Romani and Scarpa, 2000). The effect of high Mg^{2+} could be mimicked by other polyvalent cations. Fig. 1 D shows that the addition of 1 mM of the aminoglycoside antibiotic neomycin to the pipette solution almost completely inhibited the current within 5 min. Neomycin has a maximum charge of +6 at low pH and a charge of +4.5 at neutral pH (McLaughlin and Whitaker, 1988). The polyamines spermine (+4) and putrescine (+2) also inhibited but with lower potency. Dose–response experiments give 50% inhibitory concentrations (IC_{50} values) of 0.25, 0.86, and 2.4 mM for inhibition by neomycin, spermine, and putrescine, respectively, in the presence of the 2.08 mM free Mg^{2+} already in standard pipette solution (Fig. 1 E). The potency increases as the positive ionic valence increases.

Amplitude Changes of KCNQ Current Are Not Voltage Dependent

Previous studies have shown that Mg^{2+} and other polyvalent cations block some ion channels in a fast voltage-dependent manner by entering into the inner or outer

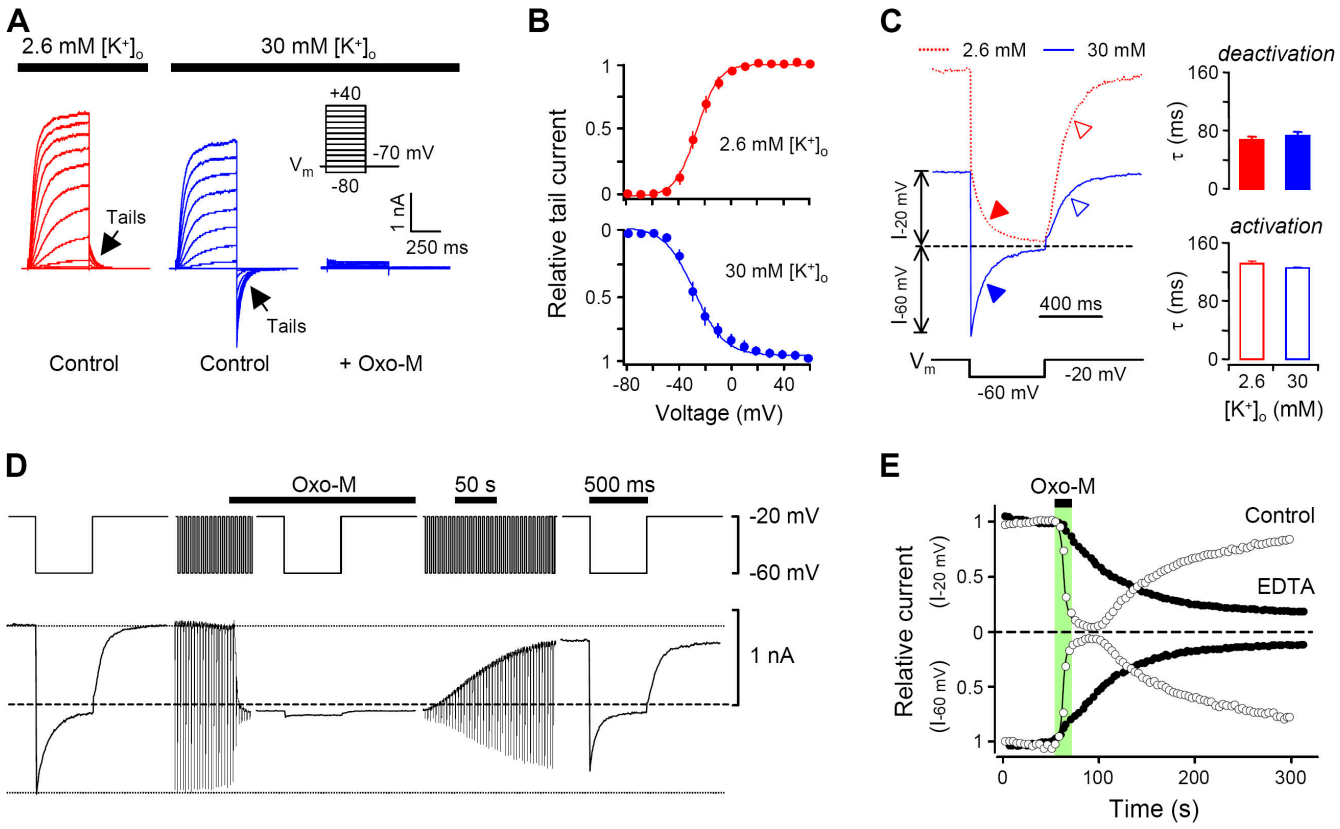

Figure 2. Inward and outward currents through KCNQ channels in high-K^+ external solution. (A) Families of voltage-clamp currents in 2.6 (normal) and 30 mM (high) K^+ solution and their suppression by 10 μM Oxo-M, from a single cell. Inset shows the pulse protocol. (B) Voltage dependence of tail currents in 2.6 and 30 mM K^+ solution. Currents are means of the data samples between 10 and 20 ms after the return to −70 mV, normalized to the maximum value. $n = 4$. (C) Current traces and mean activation and deactivation time constants during the deactivation pulse protocol in normal and high K^+ solution. Cells were dialyzed with control (5 mM Mg^{2+}) pipette solution. Right panels summarize the time constants of current activation and deactivation in the control (2.6 mM) and high K^+ (30 mM) bath solutions. (D) Reversible suppression by Oxo-M of inward and outward KCNQ currents during the deactivation pulse protocol in high K^+ solution. (E) Time course of muscarinic modulation of outward and inward currents in the high-K^+ Ringer's solution. Measurements started 3 min after breakthrough. Open circles, with normal 5 mM Mg^{2+} in pipette solution; closed circles, with Mg^{2+}-free EDTA in pipette solution. Oxo-M was applied for 20 s (bar).

mouth of the pore. For example, this is the principal mechanism of physiological inward rectification in inwardly rectifying K^+ channels (Vandenberg, 1987; Lopatin et al., 1994). There, internal polyvalent cations are drawn into the inner mouth of the pore at positive potentials, blocking outward flow of K^+, and are expelled from the inner mouth back into the cytoplasm at negative potentials, allowing inward flow of K^+. Characteristic of such block is its fast rectifying nature. Therefore we asked whether Mg^{2+} blocks current in KCNQ channels in this way by comparing the block of inward and outward K^+ currents. Increasing extracellular K^+ concentration to 30 mM raised the K^+ equilibrium potential E_K from −108 to −45 mV, so we could observe inward currents negative to −45 mV. The tail currents at −70 mV were inward (Fig. 2 A). Elevating the K^+ concentration did not change the voltage dependence of activation (Fig. 2 B; midpoints, −26.7 ± 0.5 mV in 2.6 mM K^+, −27.7 ± 1.6 mV in 30 mM K^+) or the time course of activation and deactivation (Fig. 2 C). Inward and outward currents could still be suppressed by addition of the muscarinic agonist oxotremorine-M (Oxo-M), and they recovered upon removal of Oxo-M (Fig. 2 D). Finally, the time course of muscarinic suppression of the inward and outward currents in high-K^+ solution (Fig. 2 E) was very much like the time course of suppression in standard, low-K^+ Ringer's solution (compare Suh et al., 2004), both with standard pipette solution and with the EDTA pipette solution. As we have reported before (Suh et al., 2004), muscarinic suppression of KCNQ current was extremely slow and persistent when Mg^{2+} was removed with internal EDTA, an effect we have attributed to the Mg^{2+} requirement for the G-protein cycle. Thus elevated K^+ and changes of direction of K^+ flow leave the gating and the muscarinic modulation of KCNQ channels unaltered.

Now we could test for any current rectification due to Mg^{2+}. Fig. 3 (A and B) shows that including 10 mM Mg^{2+} in the pipette decreased inward and outward KCNQ currents symmetrically, and removing Mg^{2+}

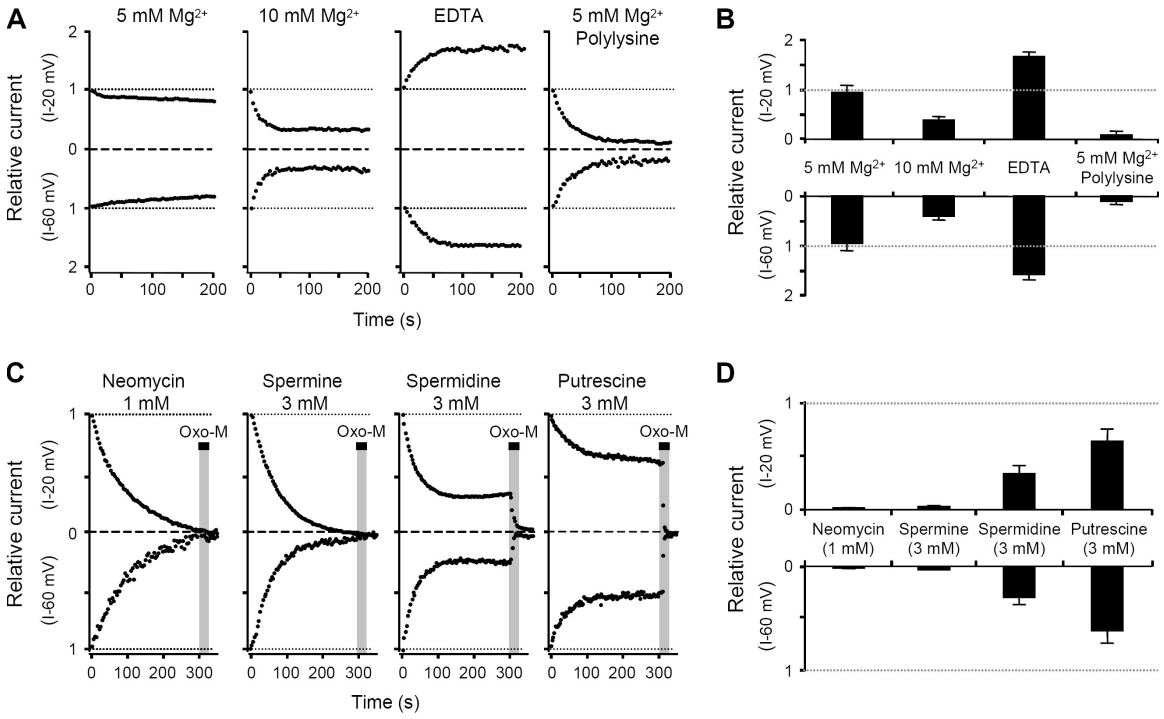

Figure 3. Symmetrical regulation of KCNQ current by intracellular Mg^{2+} and polyvalent cations. (A) Time-dependent changes of inward and outward currents in single cells dialyzed with pipette solution containing 5 mM Mg^{2+} (control), 10 mM Mg^{2+}, 1 mM EDTA without Mg^{2+} (EDTA), or 200 μM polylysine with 5 mM Mg^{2+}. The records start ($t = 0$) ~20 s after breakthrough. Dotted lines are the initial current level at −20 and −60 mV. (B) Summary of relative currents 3 min after breakthrough. Control, $n = 14$; 10 mM Mg^{2+}, $n = 8$; EDTA, $n = 10$; polylysine, $n = 3$. (C) Time-dependent changes of KCNQ current during dialysis of the indicated polyvalent cations added to the normal pipette solution (includes 5 mM Mg^{2+}). Oxo-M (10 μM) was applied after 5 min of recording. (D) Summary of relative inward and outward current levels after 5 min of intracellular dialysis with the polyamine cations neomycin ($n = 5$), spermine ($n = 5$), spermidine ($n = 6$), and putrescine ($n = 6$).

(Mg^{2+}-free EDTA) increased them symmetrically. There is no sign of voltage-dependent block or block that is dependent on the direction of current. Polylysine, a high molecular weight polybasic amine often used to sequester PIP_2, also reduced KCNQ currents symmetrically. Polylysine produces a local positive electrostatic potential when it binds to the membrane and strongly attracts and effectively sequesters multivalent PIP_2 (Wang et al., 2004). Similarly the polyamines neomycin, spermine, spermidine, and putrescine inhibited currents symmetrically (Fig. 3, C and D). These results suggest that polyvalent cations, including Mg^{2+}, do not decrease the KCNQ current by a block of the channel pore from inside the cell but instead possibly act as polylysine is assumed to act, i.e., by binding to PIP_2 electrostatically, thus reducing the availability of PIP_2 for direct interaction with the channels.

Mg^{2+} Effects Are Reversible

The actions of Mg^{2+} were readily reversible. Fig. 4 shows experiments where the same cell was patched twice by pipettes containing different Mg^{2+} concentrations. In Fig. 4 A, the first pipette with a high concentration of Mg^{2+} decreased the current and the second pipette with Mg^{2+}-free EDTA led to fast enhancement of current. In Fig. 4 B, the order is reversed with the same observation of full reversibility. These reversible changes of KCNQ current also occurred in cells treated with wortmannin (inside and outside) (Fig. 4 C), a treatment that would block the recovery of KCNQ current from muscarinic suppression by inhibiting the enzyme type III PI 4-kinase (Fig. 4 D; see also Suh and Hille, 2002; Zhang et al., 2003; Ford et al., 2004; Winks et al., 2005). That result suggests that the changes of current do not reflect degradation or synthesis of PIP_2 in the plasma membrane.

Block with Internal Mg^{2+} Differs from Block with Internal TEA

Many K^+ channels are blocked by TEA, which binds reversibly to independent sites in the outer and inner mouths of the pore (Armstrong, 1966; Hille, 1967; MacKinnon and Yellen, 1990; Holmgren et al., 1997; Hadley et al., 2000). When 30 mM TEA was included in the extracellular, high-K^+ bath solution, inward and outward KCNQ currents were symmetrically reduced ~50% without changes in the rates of activation or deactivation of the current (Fig. 5 A, also see inset). On the other hand, when the cells were dialyzed internally with TEA, there were changes both in current waveform and in rectification. With a low pipette concentration of

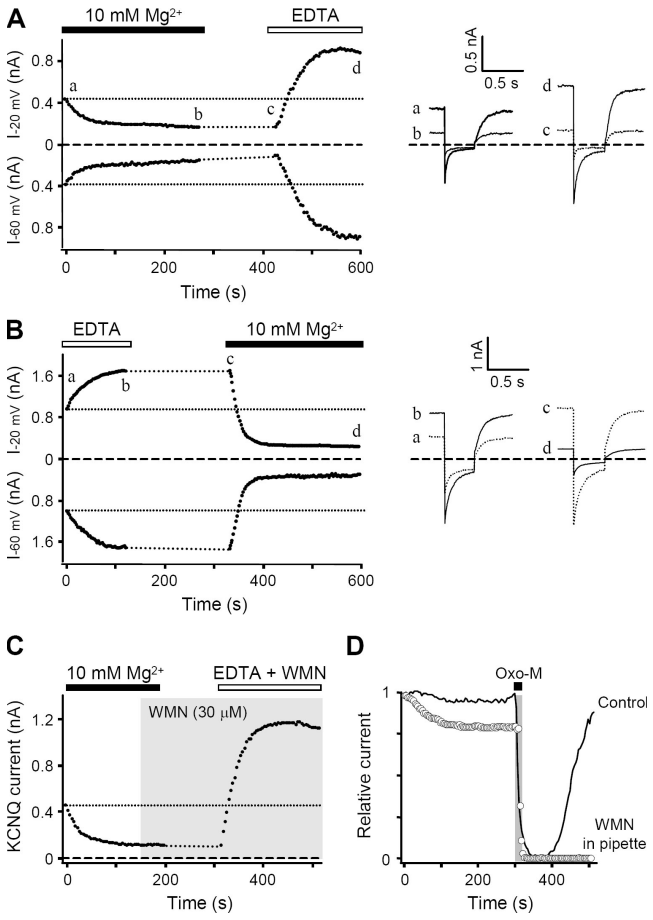

Figure 4. Intracellular Mg^{2+} reversibly regulates KCNQ current in sequential whole-cell patching. (A) Inward and outward currents in a cell dialyzed first with 10 mM Mg^{2+} and repatched with a pipette containing EDTA (Mg^{2+}-free) solution. (B) Inward and outward currents in a cell dialyzed first with Mg^{2+}-free EDTA solution and repatched with 10 mM Mg^{2+}. Thin dotted line, initial current level. Thick dotted line between points b and c, interpolated current levels during the switch of pipettes. Insets show the traces of current at the indicated time points. (C) Outward currents at −20 mV in a cell dialyzed first with 10 mM Mg^{2+} and repatched with a pipette containing EDTA (Mg^{2+}-free) and 50 μM wortmannin (WMN) in the presence of 30 μM wortmannin in bath solution. (D) Outward currents at −20 mV during intracellular dialysis with control solution (solid line) or 50 μM wortmannin (WMN) (open circle). Oxo-M was applied for 20 s (bar).

TEA (1 mM), the asymmetry was not so obvious (Fig. 5 B) but the changes in kinetics were clear (Fig. 5 C). Deactivation of the current appeared greatly slowed whereas activation appeared speeded. For comparison, we tried the KCNQ channel blocker linopirdine. It blocked outward and inward KCNQ current symmetrically when applied in the bath, and it had no action on amplitude or time course of current when applied inside (Fig. 5, D–F). Experiments with XE991 also showed that the KCNQ current was blocked only when the drug was applied outside (unpublished data). Of all the blockers we tried, only internal TEA slowed deactivation and speeded activation (Fig. 5, C and G), whereas polylysine, EDTA, high Mg^{2+}, putrescine, spermidine, and linopirdine did not (Fig. 5 G).

The action of 10 mM intracellular TEA was like the classical, open-channel block described in squid giant axons by Armstrong (1966). There the current-dependent kinetics of blocker entering and leaving the activated channel adds another transition to the gating scheme and distorts the current waveform. Fig. 6 shows that after 3 min of TEA dialysis, the inward tail current had developed a pronounced "hook" at −70 mV. The small initial size of tail current reflects the amount of channel block developed during the preceding depolarization, and the rising phase of the hook is understood as a time-dependent unblock of channels at −70 mV followed by normal deactivation gating of the unoccupied channel. The hook is larger after a depolarization to +40 mV than it is after a depolarization to −20 mV, showing that a larger fraction of channels is plugged by a TEA ion during the more positive step. Such hooks were not induced by 10 mM Mg^{2+} or polylysine in the pipette, which appear to reduce KCNQ currents by a different mechanism.

Raising Membrane PIP_2 Prevents the Modulation of KCNQ Current by Internal Mg^{2+}

Since intracellular Mg^{2+} ion can bind to the negative phosphates of PIP_2 (Hendrickson and Fullington, 1965; Toner et al., 1988), it might be reducing KCNQ current by making free PIP_2 less available. We asked if we could overcome the sensitivity to Mg^2 by augmenting PIP_2 production. Half the cells were transiently transfected with the enzyme phosphatidylinositide 4-phosphate (PIP) 5-kinase Iγ (PIPKIγ; Aikawa and Martin, 2003; see Winks et al., 2005; Suh et al., 2006), which converts PIP to PIP_2. Two groups of cells also were cotransfected with a fluorescent translocation probe, either GFP-PH_{PLC} or GFP-$C1_{PKC}$ for study with confocal microscopy. In control cells (no PIPKIγ), the GFP-PH_{PLC} probe, which binds PIP_2 and IP_3, sits at the plasma membrane (Fig. 7 A, top), whereas the GFP-$C1_{PKC}$ probe, which binds to diacylglycerol, remains in the cytoplasm (no diacylglycerol) (Fig. 7 B, top). Upon activation of PLC in control cells, the GFP-PH_{PLC} probe translocates from plasma membrane to cytoplasm, indicating significant depletion of membrane PIP_2 and production of cytoplasmic IP_3. The GFP-$C1_{PKC}$ probe translocates from cytoplasm to membrane, indicating production of diacylglycerol (GFP-$C1_{PKC}$) in the plasma membrane. Cells overexpressing both PIPKIγ and GFP-PH_{PLC} showed strong fluorescence at the plasma membrane at rest, as expected if PIP_2 is high there. However, they also showed a few very intense regions of fluorescence in the cytoplasm, suggesting formation of abnormal intracellular pools of PIP_2 by overexpressed PIPKIγ (Fig. 7 A, bottom). When cells transfected with PIPKIγ were treated with Oxo-M, the translocation of CFP-$C1_{PKC}$ was normal,

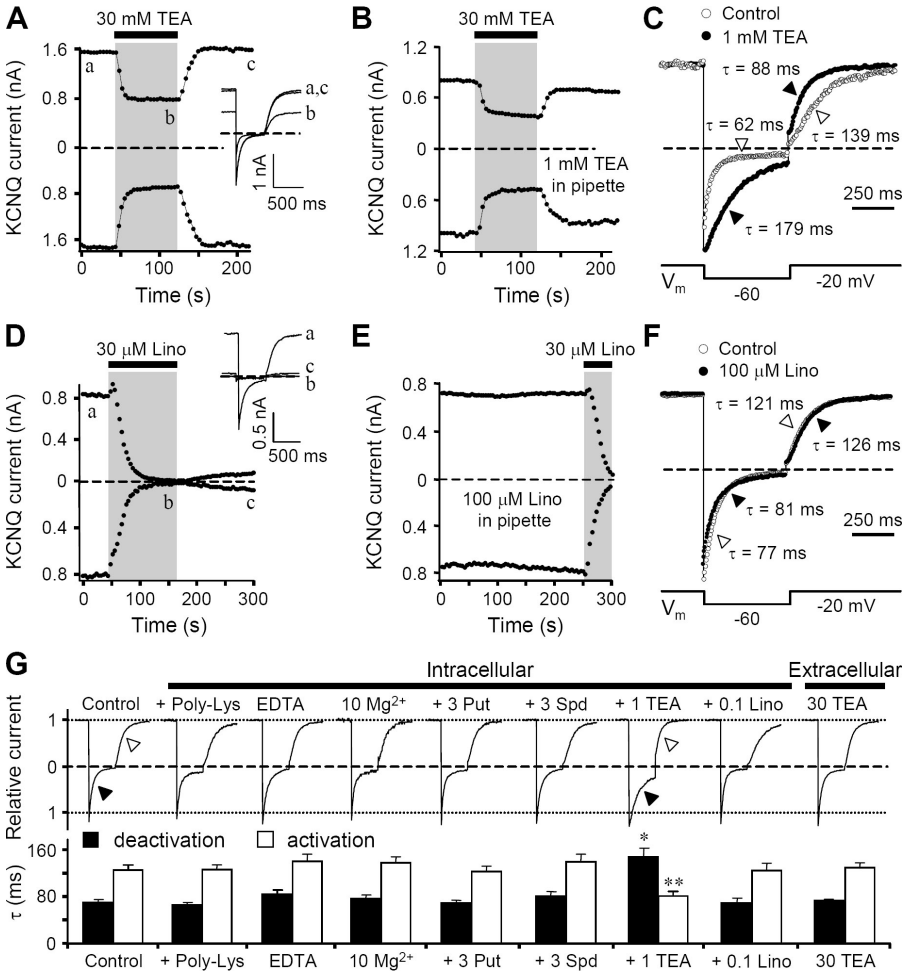

Figure 5. Intracellular TEA slows deactivation of KCNQ current. (A) Symmetrical block of inward and outward currents by extracellular TEA in high K^+ bath solution. TEA (30 mM) is applied to a cell dialyzed with control (5 mM Mg^{2+}) pipette solution. Inset shows the current waveforms where indicated. Dashed line in the current traces is the zero-current level. (B) A cell dialyzed intracellularly with 1 mM TEA also was exposed to external 30 mM TEA. Measurements started 3 min after breaking through. (C) Kinetic changes of current waveforms after dialysis with 1 mM TEA pipette in high K^+ solution compared with control. (D) Symmetrical block by 30 μM extracellular linopirdine (Lino). (E) Lack of block by intracellular dialysis with 100 μM linopirdine. The cell was treated subsequently with 30 μM extracellular linopirdine. (F) No change of current waveforms after dialysis with 100 μM intracellular linopirdine in high K^+ solution compared with control. (G) Current waveforms for cells dialyzed with different combinations of Mg^{2+}, polyamines, TEA, or inhibitors (concentrations are given in mM). The traces are normalized to the relative size of outward current. The time constants for deactivation and activation are summarized below. $n = 3$–7. *, $P < 0.01$; **, $P < 0.05$, compared with control.

whereas the translocation of the GFP-PH_{PLC} probe was only 30% of the control amount (Fig. 7, A and C). This suggested that PLC was activated and hydrolyzing PIP_2 to produce diacylglycerol normally, but because the supply of PIP_2 was so greatly augmented, the PLC reaction was not fast enough to deplete all of it (Fig. 7, B and C). From our modeling, we believe that the PIP_2 pool must have been increased many-fold by PIPKIγ (see later). Similarly modulation of KCNQ current by Oxo-M was retarded and reduced to 40% in PIPKIγ-overexpressing cells (Fig. 7 D), again implying that the PIP_2 pool was too large to be fully depleted by PLC. In other observations, PIPKIγ increased the open probability of KCNQ channels in the following ways: it shifted the voltage dependence of activation by 10 mV to more negative potentials (Fig. 7, E and F), speeded the time course of activation, and slowed deactivation of channels (Fig. 7 G).

Overexpression of PIPKIγ profoundly reduced the sensitivity of KCNQ current to changes of internal Mg^{2+}. Neither the 10 mM Mg^{2+} pipette solution nor the Mg^{2+}-free EDTA pipette solution had much effect on current (Fig. 8, A–C). In addition, PIPKIγ overexpression diminished the current inhibition by neomycin (Fig. 8, D and E). However, it did not diminish the rectifying nature of block by intracellular TEA (Fig. 8 F). Apparently current regulation by Mg^{2+}, polyamines, and PLC are attenuated by overproduction of PIP_2, whereas pore block by TEA was not changed.

DISCUSSION

We found that KCNQ2/KCNQ3 current is sensitive to the cytoplasmic free Mg^{2+} concentration. Current rises when free Mg^{2+} is lowered and falls when free Mg^{2+} is raised. The null point is near 0.47 mM free Mg^{2+}. On average the KCNQ2/3 currents in a resting cell are only 56% of what can be achieved by removing Mg^{2+}. A lack of voltage dependence of the current depression suggests that the mechanism is not a plugging of the pore from the inside. Mimicry by many polycationic amines and independence from inhibition of PI 4-kinase or PLC suggest that the mechanism does not involve changes of metabolism, especially not through Mg^{2+}-dependent enzymes nor by changing the concentration of essential Mg^{2+}–ATP complexes. Virtual elimination of the Mg^{2+} and polyvalent cation sensitivity by raising the synthesis of PIP_2 and other arguments given later favor

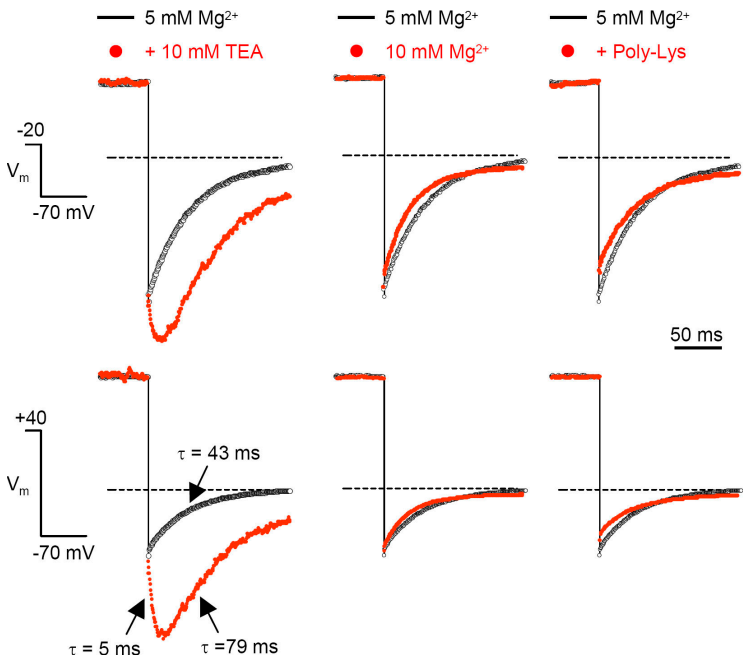

Figure 6. Hooked tail currents with TEA in the pipette. Deactivation of inward KCNQ currents at −70 mV after depolarizations to −20 or +40 mV. Cells were dialyzed with TEA (10 mM), Mg^{2+} (10 mM), or polylysine (50 μM) in high K^+ bath solution. Dashed line is the zero-current level.

a mechanism with Mg^{2+} and other polyamines interacting electrostatically with PIP_2 to reduce its availability.

As an aside to the principal theme of this paper, we also observed that intracellular TEA blocks KCNQ current by a mechanism that is distinct from the inhibition by polyvalent cations. The block by TEA follows all the rules of open-channel block as first described by Armstrong (1966) for squid delayed rectifier K^+ channels. Presumably this means that KNCQ channels have a hydrophobic inner vestibule that shares many features with other K^+ channels of the K_V family. On the other hand, linopirdine and XE991 blocked only from the outside.

Comparison with Previous Work

Intracellular Mg^{2+} is reported to reduce currents in many channels. We focus first on several well-studied cases where the channels are PIP_2 requiring and the mechanism is clearly distinct from the fast, voltage-dependent, strongly rectifying pore block found in many channels (Nowak et al., 1984; Vandenberg, 1987; Lu and MacKinnon, 1994; Voets et al., 2003; Obukhov and Nowycky, 2005; Zhang et al., 2006).

(a) An early example was the study by Chuang et al. (1997) on Kir2.3 (IRK3) channels expressed in *Xenopus* oocytes. The parallel with our KCNQ results is striking. Like us, they reported that Mg^{2+} slowly reduced current and EDTA increased current. From single-channel analysis they called the Mg^{2+} state an inactivated state. They determined a null point of 0.5 mM free Mg^{2+}, which they suggested would be the normal resting concentration in the oocyte. They also showed that activating M_1 muscarinic receptors inhibited Kir2.3 currents in a phenomenologically similar way to Mg^{2+}. Finally they proposed that activating M_1 receptors raises free Mg^{2+} as a novel second messenger acting on the channel, although no receptor mechanism that raises free Mg^{2+} was known. Subsequent work showed that activating M_1 receptors would close Kir2.3 channels by depleting PIP_2 from these PIP_2-requiring channels (Du et al., 2004), providing a different explanation for the effects of receptor activation. That study also showed that the sensitivity to Mg^{2+} was highest in versions of the channel that had the lowest PIP_2 affinity and proposed that elevated Mg^{2+} might inhibit these channels by stimulating lipid phosphatases to deplete PIP_2. However, the finding that multivalent organic cations mimic the Mg^{2+} effects in several examples means that phosphatases cannot be the general explanation for "slow" channel inhibition by polycations.

(b) Lee et al. (2005) studied slow reversible inhibition of PIP_2-dependent TRPV5 channels expressed in CHO cells. Pipette Mg^{2+} inhibited current with an IC_{50} of 0.29 mM free Mg^{2+} in whole-cell recording. With excised patches, addition of PIP_2 enhanced the current and greatly diminished the sensitivity to Mg^{2+}, whereas allowing depletion of PIP_2 reduced the current and increased the sensitivity to Mg^{2+}. In addition they found a fast, voltage-dependent block of the pore by Mg^{2+}. They suggested that the fast block involves Mg^{2+} binding to an aspartic acid in the channel, and that removal of PIP_2 could favor a slow conformational change of this Mg^{2+}-bound channel to a more persistent inhibited state.

(c) Endogenous TRPM7 channels in RBL cells are known to be PIP_2 dependent (Runnels et al., 2002) and Mg^{2+} sensitive (Nadler et al., 2001; Kozak and Cahalan, 2003). Kozak et al. (2005) found that the slow inhibition by Mg^{2+} could be mimicked by other divalent and trivalent metal cations and by all the polyvalent amine

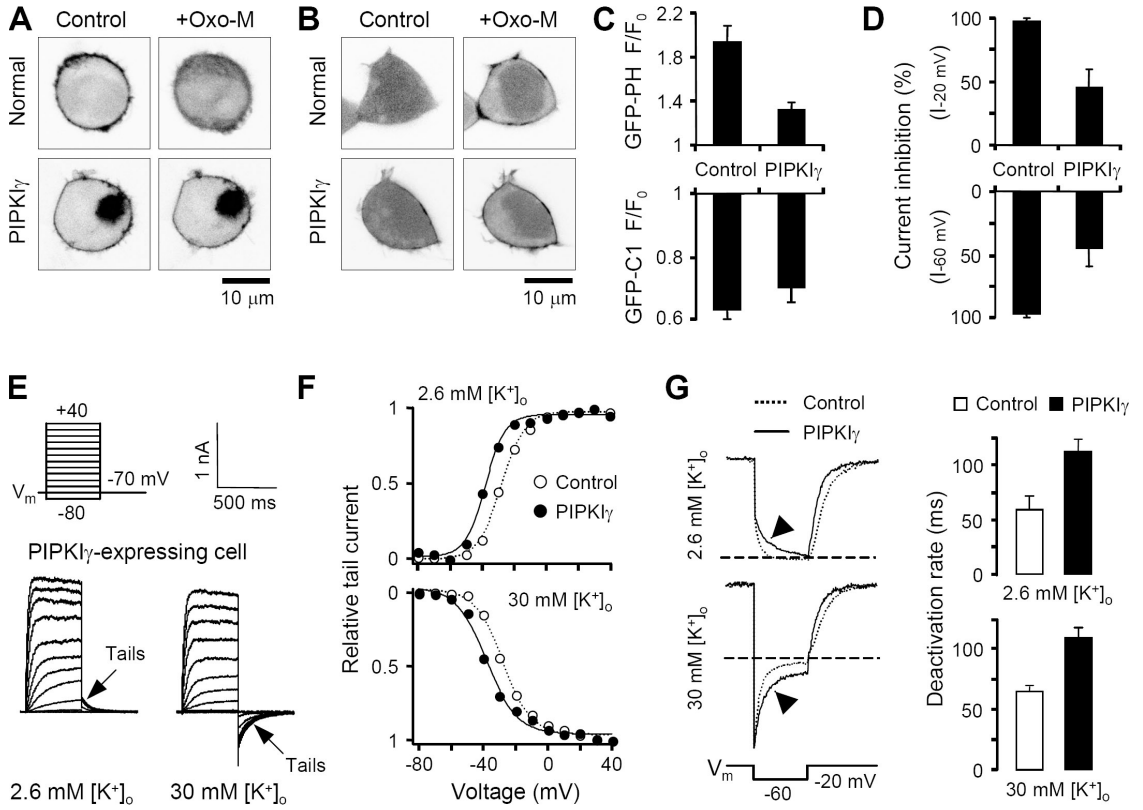

Figure 7. Overexpression of PIPKIγ attenuates receptor-mediated modulation of KCNQ current. Negative-contrast confocal images (fluorescence is dark) of the GFP-PH_{PLC} (A) and GFP-$C1_{PKC}$ (B) translocation probes transiently expressed in tsA cells with and without PIPKIγ. Images are taken before and during (at 30 s) application of 10 μM Oxo-M in the low-K bathing solution. (C) Summary of Oxo-M–induced translocation of GFP-PH_{PLC} (top) and GFP-$C1_{PKC}$ (bottom) probes in control and PIPKIγ-transfected cells (at 30 s). The fluorescence intensity of a cytoplasmic region of interest during Oxo-M treatment is normalized relative to that before. $n = 4$–5. (D) Suppression of outward and inward KCNQ current by Oxo-M in control and PIPKIγ-transfected cells in high K^+ solution. The maximum inhibition of current is given as the percentage of initial current in control ($n = 10$) and PIPKIγ-expressing ($n = 12$) cells. (E) Families of voltage-clamp currents in 2.6 mM (normal) and 30 mM (high) K^+ solution from a PIPKIγ-expressing cell. Holding potential, −20 mV, see pulse protocol. (F) Shifted voltage dependence of tail currents in PIPKIγ-expressing cells (closed circles) compared with control cells (open circles), measured in 2.6 and 30 mM K^+ solution. (G) Right, current traces for control (dotted line) and PIPKIγ-transfected (solid line) cells in normal (top) and high-K^+ (bottom) solution. Holding potential, −20 mV, see pulse protocol. Dashed line is the zero current. Left, summary of time constants for deactivation of KCNQ current without and with expression of PIPKIγ. Control, $n = 8$; PIPKIγ, $n = 5$.

cations that we tested. These cations did not induce fast voltage-dependent pore block, whereas internal TEA did. They hypothesized that Mg^{2+} might act by electrostatic screening of PIP_2. This hypothesis is very close to the one we adopt below.

(d) Finally, we mention two studies on KCNQ1/KCNE1 (IsK/KvLQT1) channels, whose suppression by activation of M_1 muscarinic receptors (Selyanko et al., 2000) suggests they have a PIP_2 requirement. Adding Mg^{2+} to the cytoplasmic side of an excised membrane patch accelerates rundown of KCNQ1/KCNE1 currents from native inner ear cells (Shen and Marcus, 1998) and expression systems (Loussouarn et al., 2003). This Mg^{2+} effect was considered not due to endogenous Mg^{2+}-dependent protein phosphatases or kinases because it was readily reversible and repeatable even while the membrane patch was bathed in a simple salt solution lacking Mg-ATP and enzymes.

Is Mg^{2+} Interacting with PIP_2?

We now consider a sequence of arguments for the hypothesis that Mg^{2+} depresses KCNQ current by reducing the availability of polyanionic PIP_2. The PIP_2 requirement for KCNQ channel function seems absolute (Suh and Hille, 2002; Zhang et al., 2003; Ford et al., 2004; Horowitz et al., 2005; Winks et al., 2005; Suh et al., 2006). When PIP_2 is removed there is no current. The Mg^{2+} ion readily forms complexes with all phosphates, especially polyphosphates. Thus the dissociation constant for the complex with inorganic HPO_4^{2-} is ∼3 mM Mg^{2+}, and those for AMP^{2-}, ADP^{3-}, and ATP^{4-} are ∼11 mM, 710 μM, and 56 μM (Martell and Sillen, 1971). (Dissociation constants for the Ba^{2+} and Ca^{2+} complexes are about the same.) PIP_2 has three phosphate groups and a maximum charge of −5 when fully ionized. PIP_2 molecules in micelles or vesicles bind at least one Mg^{2+}, and probably two, but calculation of a dissociation constant is made

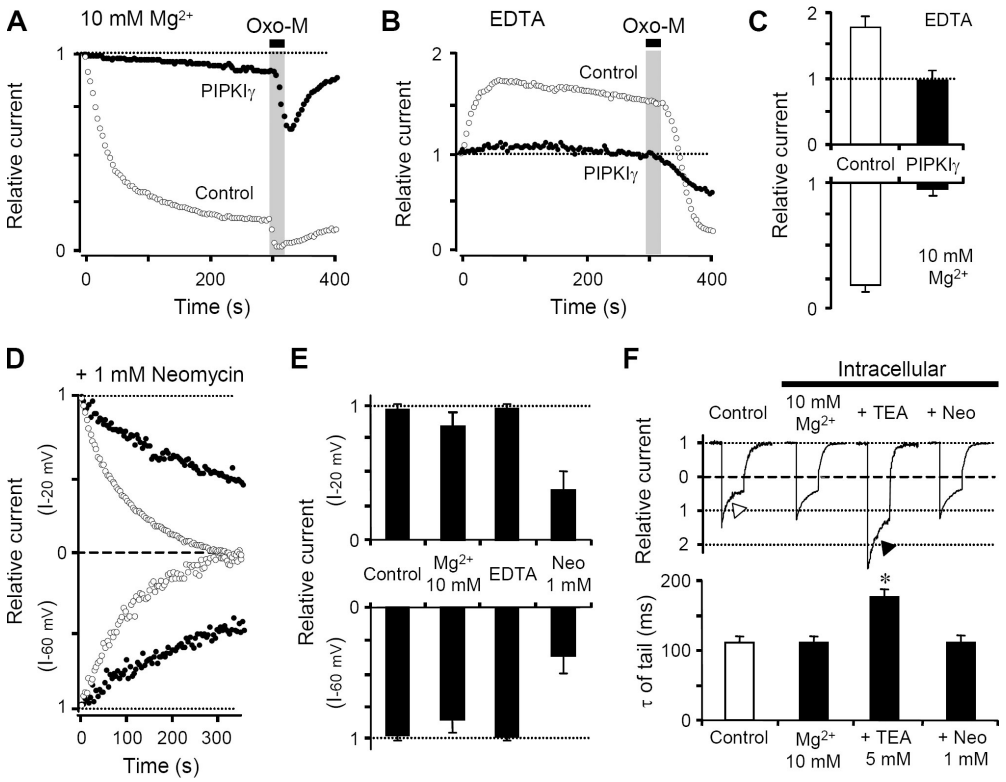

Figure 8. Overexpression of PIPKIγ attenuates Mg^{2+} sensitivity of KCNQ current. Amplitude of KCNQ current at −20 mV in control (open circle) and PIPKIγ-transfected (closed circle) cells during dialysis with 10 mM Mg^{2+} (A) or with Mg^{2+}-free EDTA (B) in the pipette. Oxo-M (10 μM) was applied for 20 s. (C) Relative current 5 min after dialysis of 10 mM Mg^{2+} or EDTA (Mg-free) in the control (open bars) and PIPKIγ-transfected (closed bars) cells. Control, $n = 14$; PIPKIγ, $n = 5$. (D) Slowed decline of current in PIPKIγ-transfected cells (closed circles) compared with control cells (open circles) during intracellular dialysis with 1 mM neomycin. The measurements start ($t = 0$) ∼20 s after breakthrough. (E) Inward and outward current 300 s after breakthrough relative to initial current in PIPKIγ-transfected cells dialyzed with different pipette solutions containing added Mg^{2+}, EDTA, or neomycin (Neo). $n = 5–15$. (F) Top, current waveforms during deactivation protocols after dialysis with Mg^{2+}, TEA (5 mM), or neomycin (1 mM, Neo) in PIPKIγ-transfected cells. Holding potential, −20 mV. The traces are normalized to the relative size of outward current. Bottom, summary of deactivation time constants (τ) after dialysis with Mg^{2+}, TEA, or neomycin. $n = 4–8$. *, $P < 0.001$, compared with control.

difficult by the negative local potential at the surface. Model-dependent numbers in the range 10 μM to 10 mM are in the literature (Hendrickson and Fullington, 1965; Toner et al., 1988). We conclude that significant binding of Mg^{2+} to membrane PIP_2 is unavoidable in the range of concentrations we studied. Formation of Mg^{2+}–PIP_2 complexes will neutralize some of the charge on PIP_2.

Does this interaction make PIP_2 less available for interaction with PIP_2-dependent proteins? We have described studies in four other channels, in addition to our work on KCNQ2/3, showing similar depression of currents by divalent metals and by a specific group of polyvalent organic cations. This similar pattern suggests that their Mg^{2+} sensitivity results from some common feature, which we suggest is their PIP_2 dependence. In each of the channels where it has been studied, clusters of basic residues in the C terminus of the channel are presumed to interact electrostatically with the three phosphate groups of PIP_2. Removing positive charges from these clusters on the channel decreases the PIP_2 affinity (Shyng et al. 2000; Du et al., 2004; Rohacs et al., 2005; Nilius et al., 2006). Adding competing polyvalent cations will diminish such electrostatic interaction between channel and PIP_2 by lowering the negative charge of the lipid. Since the true geometry of PIP_2 binding is not known for any channel, this last conclusion remains model dependent. In any case we have now shown by overexpression of the lipid kinase PIP5KIγ that the sensitivity to multivalent cations can be overcome by raising the cellular PIP_2 levels, as would be expected if the cations acted by reducing the fraction of PIP_2 available.

A confounding factor is that even if Mg^{2+} does bind to PIP_2, it necessarily interacts with many other acidic metabolites and acidic residues of proteins as well. This shows up in our assays of KCNQ current as additional components of change that we have not emphasized in this paper. For example, in Suh et al. (2004) we studied the effect of intracellular Mg^{2+} on the kinetics of muscarinic inhibition of KCNQ currents. We found that very low free Mg^{2+} severely slowed the onset of muscarinic inhibition and the recovery after inhibition (as in e.g., Fig. 2 E and Fig. 8 B of this paper). Elevated Mg^{2+} did not have large effects on inhibition. These effects were successfully described in a kinetic model for receptor-mediated inhibition in terms of known high-affinity (20 μM) Mg^{2+} requirements for the activation of G proteins, hydrolysis of GTP by G proteins, and phosphorylation and dephosphorylation of phosphoinositides by lipid kinases and phosphatases (Suh et al., 2004). While doing those experiments, we also discovered the magnesium effects elaborated in the present paper. Therefore the

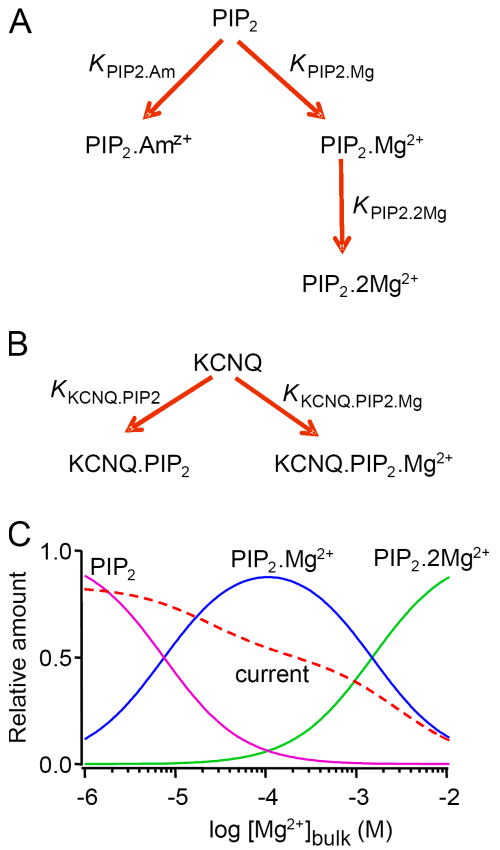

Figure 9. Model for polycation binding to PIP_2. (A) Scheme for PIP_2 interacting with the Mg^{2+} and polyvalent amines, Am^{z+}. *K*s denote dissociation constants. (B) Scheme for two forms of PIP_2 interacting with channel binding sites. (C) Calculated free and Mg^{2+}-bound forms of PIP_2 for a standard cell with total $PIP_2 = 1$ (solid lines). The fraction of total KCNQ channels with PIP_2 or PIP_2.Mg bound (dashed line) is the predicted amplitude of KCNQ current.

2004 measurements with Oxo-M were made only after 5 min of whole-cell dialysis when the amplitude changes of KCNQ current (Fig. 1 B) were nearly complete. In a higher-order analysis, the phenomena of the 2004 paper and of this paper probably do interact. The Mg^{2+} complexes with PIP_2 (and PIP) probably change the ease of hydrolysis by PLC and of phosphorylation and dephosphorylation by kinases and phosphatases and thus could affect the rates of muscarinic inhibition and recovery. Further, the direct requirement for Mg^{2+} of lipid kinases and phosphatases probably establishes new set points for the sizes of phosphoinositide pools during the experiments of this paper, giving additional slow components of relaxation of current amplitudes. For that reason, in this paper we emphasized changes that occur within 1–3 min and have not pointed to additional slower changes that might occur with long recording.

Most papers we have cited concerning an inhibition by Mg^{2+} that is not pore block, have called this "slow block." Indeed it develops over a couple of minutes during whole-cell dialysis. This time course is distinct from the fast pore block that can be induced sometimes in the same channels by for example quick steps of membrane potential. Nevertheless, the slowness may primarily reflect the speed of dialysis by diffusion from the pipette. The model we describe below attributes the block to formation of Mg^{2+} complexes with PIP_2, a process that could be intrinsically fast unless it also has to wait for dissociation of bound PIP_2 from a large reservoir of macromolecular complexes.

An Electrostatic Model

If the depression of current is as simple as forming a Mg^{2+}–PIP_2 complex, we should be able to write a simple equilibrium model. Such a model is described mathematically in the Appendix. We describe the logic here. The most elementary postulates would be that (a) Mg^{2+} and KCNQ are competing ligands for free PIP_2 in the membrane, (b) the KCNQ–PIP_2 complex can conduct current, and (c) the uncomplexed KCNQ does not conduct current. That model gives the required reversible loss of current at high Mg^{2+}, but the current would turn off much more sharply as Mg^{2+} rises than is observed. Fig. 1 C shows that the effect of Mg^{2+} develops over four decades of concentration. To rectify this discrepancy we assumed that PIP_2 binds one Mg^{2+} at low Mg^{2+} concentration, and a second Mg^{2+} at higher concentration (Fig. 9). That generates two complexes with Mg^{2+} that develop over a wider concentration range. Further, this model needs to allow the PIP_2 complex with one Mg^{2+} to bind to KCNQ channels also, but with a lower affinity than the free PIP_2 does. The line drawn in Fig. 1 C is the output of this model using constants given in Table I in the Appendix.

The next step is to consider the polyvalent amines. The dose–response curves for neomycin, spermine, and putrescine are much steeper than that for Mg^{2+}, which suggests that binding of one polyatomic, polyvalent amine suffices to "hide" a molecule of PIP_2. Therefore the model was extended to allow the polyvalent organic cations to compete with the first Mg^{2+} for free PIP_2 (Fig. 9 A). The Mg^{2+} and channel-related assumptions remain as determined before in fitting Fig. 1 C, and Mg^{2+} was included in the calculation. This model generates the three curves in Fig. 1 E. The success of the simple model shows that the concept of reduced PIP_2 availability in elevated Mg^{2+} and polyamine solutions can provide a quantitative explanation of the observations. We should point out that the null point determined here and in several published studies by patching with different free Mg^{2+} concentrations in the pipette (Fig. 1 C) may slightly overestimate the resting free Mg^{2+} of cytoplasm. This is because the starting condition (the resting cell before dialysis) includes not only the endogenous Mg^{2+} but also a significant concentration of endogenous organic polyamines (spermine and spermidine) that are normally in cytoplasm.

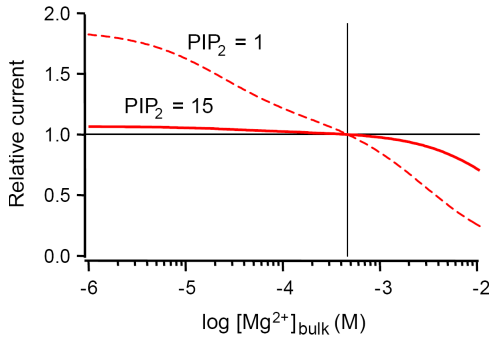

Figure 10. Reduced effect of Mg^{2+} concentration on the amplitude of KCNQ current when PIP_2 is elevated. The model was solved with PIP_2 normal ($PIP_2 = 1$) or elevated to 15. Current amplitudes were calculated from the equations for binding of PIP_2 and PIP_2. Mg to channels. Each curve is normalized to 1.0 at the estimated resting free Mg^{2+} concentration of 0.47 mM (marked by dashed lines). The actual un-normalized current is higher for elevated PIP_2 compared with $PIP_2 = 1$ at all Mg^{2+} concentrations.

Finally we consider the effect of overexpressing the lipid 5-kinase PIPKIγ, which greatly reduced the sensitivity to polyvalent cations. Presumably the total PIP_2 of those cells rose considerably as suggested in previous work (Suh et al., 2006; Winks et al., 2005) and by the reduced muscarinic suppression of M-current and of PH-domain translocation (Fig. 7, C and D). In our model, raising the total PIP_2 for example 15-fold reduces the effect of 10 mM Mg^{2+} pipettes from a 67% inhibition to a 21% inhibition, and of a 1 mM neomycin pipette, from an 80% inhibition to a 44% inhibition (see Fig. 10). Similarly, the effect of an EDTA pipette is reduced from a 78% enhancement to a 7% enhancement. These calculated effects are in qualitative agreement with the measurements in Fig. 8.

Overexpressing the lipid 5-kinase also retarded and greatly reduced the ability of Oxo-M to suppress KCNQ current and to cause translocation of the PH-domain probe (Fig. 2 E and Fig. 8 B; Suh et al., 2006; Winks et al., 2005). Qualitatively, one might anticipate difficulty in depleting PIP_2 below the thresholds for channel activation and PH-domain binding when the rate of PIP_2 production is speeded up by an order of magnitude; however, a simulation with the complete kinetic model we have used previously for simulating PIP_2 depletion by PLC (Suh et al., 2004; Horowitz et al., 2005) predicts much less slowing and reduction than is observed experimentally. This is partly because the modeled PLC reaction is fast and first order. When PIP_2 is elevated, PLC simply becomes proportionately faster. Significant improvement in the simulation is gained by assuming that the PLC reaction becomes half saturated at the normal resting PIP_2 concentration so the speeding up at higher concentration is quite limited. Further improvements can be realized by assuming "buffering" of PIP_2 concentrations from the significant abnormal intracellular pools of PIP_2 reported by the PH-domain probe, up-regulation of PI 4-kinase, or down-regulation of lipid phosphatases and PLC. Tests of these ideas are beyond the scope of this work.

Intracellular free Mg^{2+} Concentration Changes in Normal and Pathological Conditions

Changes in the concentration of intracellular ionized Mg^{2+} on cell physiology are not extensively studied and are difficult to document for the lack of a good Mg^{2+} indicator. Much intracellular Mg^{2+} is bound, so free Mg^{2+} levels represent only 2–5% of the total cellular Mg^{2+} in resting cells. Therefore, given the high concentration of metabolic intermediates or nucleotides, including Mg-ATP, in cells, it can be expected that conditions that substantially lower those levels, such as strong exercise, would also release free Mg^{2+}. For example, during ischemia in rat cardiac myocytes, free Mg^{2+} increases from 0.6–0.7 mM to 2.1–2.3 mM in parallel with the decline in ATP levels (Murphy et al., 1989b; Headrick and Willis, 1991). Possibly the cytoplasmic concentration of endogenous amines (spermine and spermidine) is subject to regulation as well. Raising their concentration would free some Mg^{2+} by competition at polyphosphates. Intracellular free Mg^{2+} also increases during transient cytoplasmic acidification (Freudenrich et al., 1992) and in hypertension (Ebel and Gunther, 2005). Whether intracellular Mg^{2+} concentration changes are used in physiological signaling is not clear, but activation of several hormonal receptors or of protein kinases with phorbol esters can alter Mg^{2+} influx and hence the level of free Mg^{2+} (Elliott and Rizack, 1974; Erdos and Maguire, 1983; Grubbs and Maguire, 1986; Maguire, 1987). Additionally the buffering capacity for Mg^{2+} may be altered by changes in metabolic state or signaling, such as local release of Ca^{2+} from the internal stores or transient change of intracellular pH, thereby altering the free Mg^{2+} concentration either globally or locally (Flatman, 1991; Murphy et al., 1991). Thus intracellular free Mg^{2+}, integrating the signals from hormone activity, cellular metabolism, and systemic ion homeostasis, could potentially regulate many Mg^{2+}-requiring enzymes and substrates as well as the free PIP_2 in cells.

Significance

We find that intracellular Mg^{2+} and polyamines inhibit KCNQ2/3, a PIP_2-requiring ion channel. Similar "slow" inhibition by polyvalent cations is seen in several other PIP_2-requiring ion channels. We find that elevated membrane PIP_2 decreases the sensitivity of KCNQ to inhibition by these cations. Conversely it is reported that partial depletion of PIP_2 increases sensitivity to inhibition by Mg^{2+} (Lee et al., 2005). Other channels, including most inward rectifier potassium (Kir) channels, TRP channels, ENaC channels, HCN channels, and probably Ca^{2+} channels, share a PIP_2 requirement (Fan and

Makielski, 1997; Kobrinsky et al., 2000; Lei et al., 2001; Gamper et al., 2004; Delmas et al., 2005; Suh and Hille, 2005; Pian et al., 2006). We suggest that all PIP_2-requiring cellular functions, including ion channels, transporters, cytoskeletal regulators, and membrane traffic components (Hilgemann et al., 2001; Suh and Hille, 2005), should exhibit sensitivity to Mg^{2+} and other polyvalent cations. This sensitivity will be less obvious for proteins that have a high affinity for PIP_2, which might remain fully PIP_2 bound even when available PIP_2 declines. It will be most obvious for proteins like KCNQ2/3 that have a low PIP_2 affinity and are only partly saturated. Such proteins may be subject to physiological regulation in conditions that change cellular polyvalent cation concentrations, and when studied in vitro, their properties including apparent PIP_2 affinity will depend on the polyvalent cation composition of the test solutions. Care should be taken to use solutions that match cellular Mg^{2+} and polycation levels in quantitative studies of any PIP_2-dependent phenomena.

APPENDIX

This Appendix describes the mathematical models for (a) the equilibrium binding of Mg^{2+} and other polycations to PIP_2 and (b) the equilibrium binding of KCNQ channel subunits to PIP_2. The rationale for the models is given in the main text.

Cation Binding to PIP_2

The scheme for binding of cations to PIP_2 is drawn in Fig. 9 A. It shows four states of PIP_2: free, complexed with one Mg^{2+}, complexed with two Mg^{2+}, and complexed with a polyamine of valence $z+$. The equilibrium constants K indicated by each arrow are dissociation constants in units of molar. We use conventional equations for multiple simultaneous equilibrium binding. If a is the total PIP_2 concentration relative to that in a standard cell, and Mg and Am^{z+} are the local concentrations of the Mg^{2+} and polyamine ligands in the vicinity of the PIP_2, the solution of this equilibrium for a standard cell is given by: $a = 1$; $b = a \times Mg/K_{PIP2.Mg}$; $c = b \times Mg/K_{PIP2.2Mg}$; $d = a \times Am^{z+}/K_{PIP2.Amz+}$; $D = a + b + c + d$; $PIP_2 = a/D$; $PIP_2.Mg = b/D$; $PIP_2.2Mg = c/D$; $PIP_2.Am^{z+} = d/D$. When $a = 1$, i.e., with a standard resting amount of total PIP_2, the calculated values for PIP_2, $PIP_2.Mg$, $PIP_2.2Mg$, and $PIP_2.Am^{z+}$ are numerically equal to the fraction of PIP_2 in each of the four forms. When neither Mg^{2+} nor organic polyamines are present, the free PIP_2 would then be $PIP_2 = 1$.

The model also assumes that there is a local negative potential ψ at the cation binding site. This local potential raises the local cationic ligand concentration by an equilibrium Boltzmann factor that depends on the valence of the cation: $Mg = [Mg^{2+}]_{bulk}\exp(-2q_e\psi/kT)$ and $Am^{z+} = [Am^{z+}]_{bulk}\exp(-zq_e\psi/kT)$, where q_e, k, and T are the charge of an electron, Boltzmann's constant, and the absolute temperature, respectively. This assumption of a local negativity is not required to make a workable model, but it was invoked because the region around a PIP_2, with its three phosphate groups, will certainly be negative, and it gives a natural explanation for why the apparent affinity of polyvalent cations increases with the charge of the cation.

TABLE I
Three Alternative Solutions of the Binding Model

	Local potential		
	0 mV	−15 mV	−40 mV
$K_{PIP2.Mg}$	8 μM	27 μM	196 μM
$K_{PIP2.2Mg}$	1.2 mM	4 mM	29 mM
$K_{PIP2.putrescine}$	3 μM	10 μM	74 μM
$K_{PIP2.spermine}$	0.9 μM	10 μM	550 μM
$K_{PIP2.neomycin}$	0.27 μM	10 μM	4 mM

Table I shows values of constants that predict the concentration dependence for Mg^{2+} binding illustrated in Fig. 9 C. There is a 150-fold separation of the two Mg^{2+} binding steps on the concentration axis. The three sets of dissociation constants appropriate for different local potentials give the same binding curves.

Binding of PIP_2 Species to KCNQ Subunits

The purpose of the model was to simulate the depression of KCNQ current by the addition of cytoplasmic polyvalent cations. Allowing both free PIP_2 and singly occupied $PIP_2.Mg$ to bind to channels as diagramed in Fig. 9 B allowed us to achieve the broad dose–response curve seen empirically (Fig. 1 C). The equations take the same format as those for PIP_2–polycation interaction: $f = 1$; $g = f \times PIP_2/K_{KCNQ.PIP2}$; $h = f \times PIP_2.Mg/K_{KCNQ.PIP2.Mg}$; $D = f + g + h$; $KCNQ = f/D$; $KCNQ.PIP_2.Mg = g/D$; $KCNQ.PIP_2.2Mg = h/D$. The dissociation constants were chosen as $K_{KCNQ.PIP2} = 0.2$ and $K_{KCNQ.PIP2.Mg} = 1.0$. These numbers are dimensionless, where 0.2 means that the channel would be half saturated when 20% of the standard PIP_2 is free. The broad, predicted dose–response curve for Mg^{2+} experiments is drawn as a solid line in Fig. 1 C and as a dashed line in Fig. 9 C. The predicted dose–response curves for experiments with neomycin, spermine, and putrescine are drawn as solid lines in Fig. 1 E. In this latter calculation, the concentration of individual polyamines is varied in the constant presence of 2 mM free Mg^{2+} to mimic the conditions of the actual experiments. The cations were assumed to be fully ionized at the local pH near the binding site, which would be a little more acidic than that of the cytoplasmic solution when there is a negative surface potential.

Effect of Elevated PIP_2

The simulation of the effect of overexpressing PIPKIγ described in text was done by elevating the PIP_2 concentration from the standard value of 1 to 15 in the binding

model. Fig. 10 shows that the dose–response curve for Mg^{2+} acting on current becomes nearly flat.

Discussion of the Binding Model

This model is simplified in several respects. One simplification is that the polyvalent ions are assumed only to form chemical complexes with PIP_2 rather than to both screen surface negative charge of the membrane and bind to PIP_2 in the sense of the Gouy-Chapman-Stern double-layer model used by Toner et al. (1988). If the local potential is small, the double-layer screening effects would not be strong; however to model large potentials such as −40 mV, a full Gouy-Chapman-Stern treatment would be proper. The assumption that up to 2 Mg^{2+} ions can bind per PIP_2 is not a new one. It was used by Hendrickson and Fullington (1965) and Toner et al. (1988). Our model gives quite different dissociation constants depending on the assumed local potential. The two intrinsic Mg^{2+} dissociation constants in the model of Toner et al. are on the order of 2 and 10 mM at their zeta potential of −38 mV. These considerations point to how model dependent the values of such parameters are. The success of our model shows that direct binding of polyvalent cations to PIP_2 can explain the depression of K^+ currents, but a range of formulations and specific parameter values probably would work.

A second simplification is that the current is directly proportional to the fraction of channels with a bound PIP_2 or PIP_2.Mg. Presumably in fact the four subunits of KCNQ channels each can bind one or several molecules of phosphoinositide, and the activity of channel tetramers might be more complicated than just a linear function of occupancy.

A third simplification is that the cation-binding scheme of Fig. 9 A is solved first and then the channel-binding scheme of Fig. 9 B is solved assuming that it does not perturb the population of cation-binding states. This is equivalent to saying that the number of channels is much less than the number of PIP_2 molecules. The kinetic model we have used in the past for PIP_2 metabolism assumes that there are 5,000 PIP_2 molecules per square micrometer in a standard cell at rest. As an order-of-magnitude calculation, we note that the highest current density observed in our experiments (100 pA/pF) is equivalent to 1 pA/μm^2. Only one or two open channels per square micrometer is needed for that current.

We thank Lea Miller for technical assistance, Greg Martin in the Keck Center for Neural Imaging for help with microscopy, and Drs. Y. Aikawa and T.F. Martin for the PIPKIγ construct.

This work was supported by National Institutes of Health grant NS08174 from the National Institute of Neurological Disorders and Stroke.

Edward N. Pugh Jr. served as editor.

Submitted: 15 May 2007
Accepted: 1 August 2007

REFERENCES

Aikawa, Y., and T.F. Martin. 2003. ARF6 regulates a plasma membrane pool of phosphatidylinositol 4,5-bisphosphate required for regulated exocytosis. *J. Cell Biol.* 162:647–659.

Alvarez-Leefmans, F.J., F. Giraldez, and S.M. Gamino. 1987. Intracellular free magnesium in excitable cells: its measurement and its biologic significance. *Can. J. Physiol. Pharmacol.* 65:915–925.

Armstrong, C.M. 1966. Time course of TEA^+-induced anomalous rectification in squid giant axons. *J. Gen. Physiol.* 50:491–503.

Bernheim, L., A. Mathie, and B. Hille. 1992. Characterization of muscarinic receptor subtypes inhibiting Ca^{2+} current and M current in rat sympathetic neurons. *Proc. Natl. Acad. Sci. USA.* 89:9544–9548.

Brocard, J.B., S. Rajdev, and I.J. Reynolds. 1993. Glutamate-induced increases in intracellular free Mg^{2+} in cultured cortical neurons. *Neuron.* 11:751–757.

Brown, D.A. 1988. M currents. *Ion Channels.* 1:55–94.

Chuang, H., Y.N. Jan, and L.Y. Jan. 1997. Regulation of IRK3 inward rectifier K^+ channel by M_1 acetylcholine receptor and intracellular magnesium. *Cell.* 89:1121–1132.

Delmas, P., and D.A. Brown. 2005. Pathways modulating neural KCNQ/M (K_v7) potassium channels. *Nat. Rev. Neurosci.* 6:850–862.

Delmas, P., B. Coste, N. Gamper, and M.S. Shapiro. 2005. Phosphoinositide lipid second messengers: new paradigms for calcium channel modulation. *Neuron.* 47:179–182.

Downing, G.J., S. Kim, S. Nakanishi, K.J. Catt, and T. Balla. 1996. Characterization of a soluble adrenal phosphatidylinositol 4-kinase reveals wortmannin sensitivity of type III phosphatidylinositol kinases. *Biochemistry.* 35:3587–3594.

Du, X., H. Zhang, C. Lopes, T. Mirshahi, T. Rohacs, and D.E. Logothetis. 2004. Characteristic interactions with phosphatidylinositol 4,5-bisphosphate determine regulation of kir channels by diverse modulators. *J. Biol. Chem.* 279:37271–37281.

Ebel, H., and T. Gunther. 2005. Na^+/Mg^{2+} antiport in erythrocytes of spontaneously hypertensive rats: role of Mg^{2+} in the pathogenesis of hypertension. *Magnes. Res.* 18:175–185.

Elliott, D.A., and M.A. Rizack. 1974. Epinephrine and adrenocorticotropic hormone-stimulated magnesium accumulation in adipocytes and their plasma membranes. *J. Biol. Chem.* 249:3985–3990.

Erdos, J.J., and M.E. Maguire. 1983. Hormone-sensitive magnesium transport in murine S49 lymphoma cells: characterization and specificity for magnesium. *J. Physiol.* 337:351–371.

Fan, Z., and J.C. Makielski. 1997. Anionic phospholipids activate ATP-sensitive potassium channels. *J. Biol. Chem.* 272:5388–5395.

Flatman, P.W. 1991. Mechanisms of magnesium transport. *Annu. Rev. Physiol.* 53:259–271.

Ford, C.P., P.L. Stemkowski, and P.A. Smith. 2004. Possible role of phosphatidylinositol 4,5-bisphosphate in luteinizing hormone releasing hormone-mediated M-current inhibition in bullfrog sympathetic neurons. *Eur. J. Neurosci.* 20:2990–2998.

Freudenrich, C.C., E. Murphy, L.A. Levy, R.E. London, and M. Lieberman. 1992. Intracellular pH modulates cytosolic free magnesium in cultured chicken heart cells. *Am. J. Physiol.* 262: C1024–C1030.

Gamper, N., V. Reznikov, Y. Yamada, J. Yang, and M.S. Shapiro. 2004. Phosphatidylinositol 4,5-bisphosphate signals underlie receptor-specific $G_{q/11}$-mediated modulation of N-type Ca^{2+} channels. *J. Neurosci.* 24:10980–10992.

Gilman, A.G. 1987. G proteins: transducers of receptor-generated signals. *Annu. Rev. Biochem.* 56:615–649.

Gotoh, H., M. Kajikawa, H. Kato, and K. Suto. 1999. Intracellular Mg^{2+} surge follows Ca^{2+} increase during depolarization in cultured neurons. *Brain Res.* 828:163–168.

Grubbs, R.D., and M.E. Maguire. 1986. Regulation of magnesium but not calcium transport by phorbol ester. *J. Biol. Chem.* 261:12550–12554.

Gupta, R.K., P. Gupta, and R.D. Moore. 1984. NMR studies of intracellular metal ions in intact cells and tissues. *Annu. Rev. Biophys. Bioeng.* 13:221–246.

Hadley, J.K., M. Noda, A.A. Selyanko, I.C. Wood, F.C. Abogadie, and D.A. Brown. 2000. Differential tetraethylammonium sensitivity of KCNQ1-4 potassium channels. *Br. J. Pharmacol.* 129:413–415.

Headrick, J.P., and R.J. Willis. 1991. Cytosolic free magnesium in stimulated, hypoxic, and underperfused rat heart. *J. Mol. Cell. Cardiol.* 23:991–999.

Hendrickson, H.S., and J.G. Fullington. 1965. Stabilities of metal complexes of phospholipids: Ca^{2+}, Mg^{2+}, and Ni^{2+} complexes of phosphatidylserine and triphosphoinositide. *Biochemistry.* 4:1599–1605.

Hilgemann, D.W., S. Feng, and C. Nasuhoglu. 2001. The complex and intriguing lives of PIP_2 with ion channels and transporters. *Sci. STKE.* 2001:RE19.

Hille, B. 1967. The selective inhibition of delayed potassium currents in nerve by tetraethylammonium ion. *J. Gen. Physiol.* 50:1287–1302.

Holmgren, M., P.L. Smith, and G. Yellen. 1997. Trapping of organic blockers by closing of voltage-dependent K^+ channels: evidence for a trap door mechanism of activation gating. *J. Gen. Physiol.* 109:527–535.

Horowitz, L.F., W. Hirdes, B.C. Suh, D.W. Hilgemann, K. Mackie, and B. Hille. 2005. Phospholipase C in living cells: activation, inhibition, Ca^{2+} requirement, and regulation of M current. *J. Gen. Physiol.* 126:243–262.

Jones, S., D.A. Brown, G. Milligan, E. Willer, N.J. Buckley, and M.P. Caulfield. 1995. Bradykinin excites rat sympathetic neurons by inhibition of M current through a mechanism involving B2 receptors and $G\alpha_{q/11}$. *Neuron.* 14:399–405.

Kobrinsky, E., T. Mirshahi, H. Zhang, T. Jin, and D.E. Logothetis. 2000. Receptor-mediated hydrolysis of plasma membrane messenger PIP_2 leads to K^+ current desensitization. *Nat. Cell Biol.* 2:507–514.

Kozak, J.A., and M.D. Cahalan. 2003. MIC channels are inhibited by internal divalent cations but not ATP. *Biophys. J.* 84:922–927.

Kozak, J.A., M. Matsushita, A.C. Nairn, and M.D. Cahalan. 2005. Charge screening by internal pH and polyvalent cations as a mechanism for activation, inhibition, and rundown of TRPM7/MIC channels. *J. Gen. Physiol.* 126:499–514.

Kubota, T., Y. Shindo, K. Tokuno, H. Komatsu, H. Ogawa, S. Kudo, Y. Kitamura, K. Suzuki, and K. Oka. 2005. Mitochondria are intracellular magnesium stores: investigation by simultaneous fluorescent imagings in PC12 cells. *Biochim. Biophys. Acta.* 1744:19–28.

Lee, J., S.K. Cha, T.J. Sun, and C.L. Huang. 2005. PIP_2 activates TRPV5 and releases its inhibition by intracellular Mg^{2+}. *J. Gen. Physiol.* 126:439–451.

Lei, Q., E.M. Talley, and D.A. Bayliss. 2001. Receptor-mediated inhibition of G protein-coupled inwardly rectifying potassium channels involves $G\alpha_q$ family subunits, phospholipase C, and a readily diffusible messenger. *J. Biol. Chem.* 276:16720–16730.

Lerche, H., Y.G. Weber, K. Jurkat-Rott, and F. Lehmann-Horn. 2005. Ion channel defects in idiopathic epilepsies. *Curr. Pharm. Des.* 11:2737–2752.

London, R.E. 1991. Methods for measurement of intracellular magnesium: NMR and fluorescence. *Annu. Rev. Physiol.* 53:241–258.

Lopatin, A.N., E.N. Makhina, and C.G. Nichols. 1994. Potassium channel block by cytoplasmic polyamines as the mechanism of intrinsic rectification. *Nature.* 372:366–369.

Loussouarn, G., K.H. Park, C. Bellocq, I. Baro, F. Charpentier, and D. Escande. 2003. Phosphatidylinositol 4,5-bisphosphate, PIP_2, controls KCNQ1/KCNE1 voltage-gated potassium channels: a functional homology between voltage-gated and inward rectifier K^+ channels. *EMBO J.* 22:5412–5421.

Lu, Z., and R. MacKinnon. 1994. Electrostatic tuning of Mg^{2+} affinity in an inward-rectifier K^+ channel. *Nature.* 371:243–246.

MacKinnon, R., and G. Yellen. 1990. Mutations affecting TEA blockade and ion permeation in voltage-activated K^+ channels. *Science.* 250:276–279.

Maguire, M.E. 1987. Hormonal regulation of magnesium uptake: differential coupling of membrane receptors to magnesium uptake. *Magnesium.* 6:180–191.

Marrion, N.V., T.G. Smart, S.J. Marsh, and D.A. Brown. 1989. Muscarinic suppression of the M-current in the rat sympathetic ganglion is mediated by receptors of the M_1-subtype. *Br. J. Pharmacol.* 98:557–573.

Martell, A.E., and L.G. Sillen. 1971. Stability constants of metal-ion complexes. Supplement 1. Special Publ., 25. The Chemical Society, London. 108 and 652.

McLaughlin, S., and M. Whitaker. 1988. Cations that alter surface potentials of lipid bilayers increase the calcium requirement for exocytosis in sea urchin eggs. *J. Physiol.* 396:189–204.

Murphy, E., C.C. Freudenrich, and M. Lieberman. 1991. Cellular magnesium and Na/Mg exchange in heart cells. *Annu. Rev. Physiol.* 53:273–287.

Murphy, E., C.C. Freudenrich, L.A. Levy, R.E. London, and M. Lieberman. 1989a. Monitoring cytosolic free magnesium in cultured chicken heart cells by use of the fluorescent indicator Furaptra. *Proc. Natl. Acad. Sci. USA.* 86:2981–2984.

Murphy, E., C. Steenbergen, L.A. Levy, B. Raju, and R.E. London. 1989b. Cytosolic free magnesium levels in ischemic rat heart. *J. Biol. Chem.* 264:5622–5627.

Nadler, M.J., M.C. Hermosura, K. Inabe, A.L. Perraud, Q. Zhu, A.J. Stokes, T. Kurosaki, J.P. Kinet, R. Penner, A.M. Scharenberg, and A. Fleig. 2001. LTRPC7 is a Mg·ATP-regulated divalent cation channel required for cell viability. *Nature.* 411:590–595.

Nilius, B., F. Mahieu, J. Prenen, A. Janssens, G. Owsianik, R. Vennekens, and T. Voets. 2006. The Ca^{2+}-activated cation channel TRPM4 is regulated by phosphatidylinositol 4,5-biphosphate. *EMBO J.* 25:467–478.

Nowak, L., P. Bregestovski, P. Ascher, A. Herbet, and A. Prochiantz. 1984. Magnesium gates glutamate-activated channels in mouse central neurones. *Nature.* 307:462–465.

Obukhov, A.G., and M.C. Nowycky. 2005. A cytosolic residue mediates Mg^{2+} block and regulates inward current amplitude of a transient receptor potential channel. *J. Neurosci.* 25:1234–1239.

Pian, P., A. Bucchi, R.B. Robinson, and S.A. Siegelbaum. 2006. Regulation of gating and rundown of HCN hyperpolarization-activated channels by exogenous and endogenous PIP_2. *J. Gen. Physiol.* 128:593–604.

Rohacs, T., C.M. Lopes, I. Michailidis, and D.E. Logothetis. 2005. $PI(4,5)P_2$ regulates the activation and desensitization of TRPM8 channels through the TRP domain. *Nat. Neurosci.* 8:626–634.

Romani, A., and A. Scarpa. 2000. Regulation of cellular magnesium. *Front. Biosci.* 5:D720–D734.

Runnels, L.W., L. Yue, and D.E. Clapham. 2002. The TRPM7 channel is inactivated by PIP_2 hydrolysis. *Nat. Cell Biol.* 4:329–336.

Schlingmann, K.P., S. Weber, M. Peters, L. Niemann Nejsum, H. Vitzthum, K. Klingel, M. Kratz, E. Haddad, E. Ristoff, D. Dinour, et al. 2002. Hypomagnesemia with secondary hypocalcemia is caused by mutations in TRPM6, a new member of the TRPM gene family. *Nat. Genet.* 31:166–170.

Schmitz, C., A.L. Perraud, C.O. Johnson, K. Inabe, M.K. Smith, R. Penner, T. Kurosaki, A. Fleig, and A.M. Scharenberg. 2003. Regulation of vertebrate cellular Mg^{2+} homeostasis by TRPM7. *Cell.* 114:191–200.

Selyanko, A.A., J.K. Hadley, I.C. Wood, F.C. Abogadie, T.J. Jentsch, and D.A. Brown. 2000. Inhibition of KCNQ1-4 potassium channels expressed in mammalian cells via M_1 muscarinic acetylcholine receptors. *J. Physiol.* 522:349–355.

Shen, Z., and D.C. Marcus. 1998. Divalent cations inhibit IsK/KvLQT1 channels in excised membrane patches of strial marginal cells. *Hear. Res.* 123:157–167.

Suh, B.C., and B. Hille. 2002. Recovery from muscarinic modulation of M current channels requires phosphatidylinositol 4,5-bisphosphate synthesis. *Neuron.* 35:507–520.

Suh, B.C., and B. Hille. 2005. Regulation of ion channels by phosphatidylinositol 4,5-bisphosphate. *Curr. Opin. Neurobiol.* 15:370–378.

Suh, B.C., L.F. Horowitz, W. Hirdes, K. Mackie, and B. Hille. 2004. Regulation of KCNQ2/KCNQ3 current by G protein cycling: the kinetics of receptor-mediated signaling by G_q. *J. Gen. Physiol.* 123:663–683.

Suh, B.C., T. Inoue, T. Meyer, and B. Hille. 2006. Rapid chemically induced changes of PtdIns(4,5)P_2 gate KCNQ ion channels. *Science.* 314:1454–1457.

Suzuki, T., Y. Banno, and Y. Nozawa. 1991. Partial purification and characterization of two forms of phosphatidylinositol 4-phosphate 5-kinase from human platelet membrane. *Thromb. Res.* 64:45–56.

Shyng, S.L., C.A. Cukras, J. Harwood, and C.G. Nichols. 2000. Structural determinants of PIP_2 regulation of inward rectifier K_{ATP} channels. *J. Gen. Physiol.* 116:599–608.

Takaya, J., H. Higashino, R. Miyazaki, and Y. Kobayashi. 1998. Effects of insulin and insulin-like growth factor-1 on intracellular magnesium of platelets. *Exp. Mol. Pathol.* 65:104–109.

Toner, M., G. Vaio, A. McLaughlin, and S. McLaughlin. 1988. Adsorption of cations to phosphatidylinositol 4,5-bisphosphate. *Biochemistry.* 27:7435–7443.

Vandenberg, C.A. 1987. Inward rectification of a potassium channel in cardiac ventricular cells depends on internal magnesium ions. *Proc. Natl. Acad. Sci. USA.* 84:2560–2564.

Voets, T., A. Janssens, J. Prenen, G. Droogmans, and B. Nilius. 2003. Mg^{2+}-dependent gating and strong inward rectification of the cation channel TRPV6. *J. Gen. Physiol.* 121:245–260.

Voets, T., B. Nilius, S. Hoefs, A.W. van der Kemp, G. Droogmans, R.J. Bindels, and J.G.J. Hoenderop. 2004. TRPM6 forms the Mg^{2+} influx channel involved in intestinal and renal Mg^{2+} absorption. *J. Biol. Chem.* 279:19–25.

Walder, R.Y., D. Landau, P. Meyer, H. Shalev, M. Tsolia, Z. Borochowitz, M.B. Boettger, G.E. Beck, R.K. Englehardt, R. Carmi, and V.C. Sheffield. 2002. Mutation of TRPM6 causes familial hypomagnesemia with secondary hypocalcemia. *Nat. Genet.* 31:171–174.

Wang, J., A. Gambhir, S. McLaughlin, and D. Murray. 2004. A computational model for the electrostatic sequestration of PI(4,5)P_2 by membrane-adsorbed basic peptides. *Biophys. J.* 86:1969–1986.

White, R.E., and H.C. Hartzell. 1989. Magnesium ions in cardiac function. Regulator of ion channels and second messengers. *Biochem. Pharmacol.* 38:859–867.

Winks, J.S., S. Hughes, A.K. Filippov, L. Tatulian, F.C. Abogadie, D.A. Brown, and S.J. Marsh. 2005. Relationship between membrane phosphatidylinositol 4,5-bisphosphate and receptor-mediated inhibition of native neuronal M channels. *J. Neurosci.* 25:3400–3413.

Yamakawa, A., and T. Takenawa. 1988. Purification and characterization of membrane-bound phosphatidylinositol kinase from rat brain. *J. Biol. Chem.* 263:17555–17560.

Zhang, H., L.C. Craciun, T. Mirshahi, T. Rohacs, C.M. Lopes, T. Jin, and D.E. Logothetis. 2003. PIP_2 activates KCNQ channels and its hydrolysis underlies receptor-mediated inhibition of M currents. *Neuron.* 37:963–975.

Zhang, Y., X. Niu, T.I. Brelidze, and K.L. Magleby. 2006. Ring of negative charge in BK channels facilitates block by intracellular Mg^{2+} and polyamines through electrostatics. *J. Gen. Physiol.* 128:185–202.